DOI: 10.1002/ejic.200700879

# Indenylidene-Ruthenium Complexes Bearing Saturated N-Heterocyclic Carbenes: Synthesis and Catalytic Investigation in Olefin Metathesis Reactions

**Stijn Monsaert,[a] Renata Drozdzak,*[a] Valerian Dragutan,[b] Ileana Dragutan,[b] and Francis Verpoort*[a]**

**Keywords:** Carbene ligands / Homogeneous catalysis / Metathesis / N-Heterocyclic carbenes / Ruthenium

The synthesis of complexes of the general formula $Cl_2Ru$-(SIMes)(L)(3-phenylinden-1-ylidene) (**5**, L = $PCy_3$; **6**, L = py; and **7**, L = $PPh_3$) from $Cl_2Ru(PR_3)_2$(3-phenylinden-1-ylidene) (**2a**, R = Ph; **2b**, R = Cy) is reported. This family of olefin metathesis catalysts was fully characterized ($^1H$, $^{13}C$ and $^{31}P$ NMR spectroscopy and elemental analysis) and provided excellent activity in the ring-opening metathesis polymerization of 1,5-cyclooctadiene and the ring-closing metathesis of diethyl diallylmalonate. Comparison with the corresponding benzylidene-containing catalysts, **1a**,**c** and **8b**, established the decisive role of the carbene ligand on the procedure of the reaction and led to the observation of an unusual catalytic phenomenon, here called "self-inhibition".



## Introduction

In recent years olefin metathesis, as a powerful, atom-efficient, synthetic strategy for C–C-bond forming, has met with great success, mainly because of outstanding advances in catalyst performance.[1] In the quest for better catalysts, the class of Ru-indenylidene[2] complexes with different ancillary ligands was also investigated, and compared to the Ru-benzylidene Grubbs' catalysts (**1a**–**c**, Scheme 1).[3] It was evidenced that all indenylidene ruthenium catalysts display higher thermal stability than their benzylidene counterparts, which obviously translates into longer lifetimes. In addition, good catalytic activities in RCM[2b,2l] and ROMP[2g,2h] have been reported. Among olefin metathesis catalysts, the combined high catalyst stability and activity is a unique beneficial feature of indenylidenes.

Introduction of the sterically demanding NHC ligands into Ru complexes was an important milestone on the metathesis road of success.[2b,3c–3g,4] The logical approach to further advancement in the indenylidene series along these lines, that is, ligand exchange in **2** with an unsaturated NHC moiety (IMes and IPr), was first achieved by Nolan[2b] through synthesis of complexes **3a**–**d**. In view of the improved performance of SIMes- versus IMes-Ru-benzylidene catalysts, it is surprising that to date no reports have been published on the parent complexes bearing saturated NHC

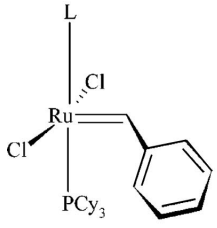


**1a** L = $PCy_3$
**1b** L = IMes
**1c** L = SIMes

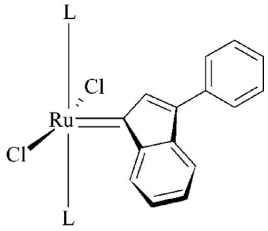


**2a** L = $PPh_3$
**2b** L = $PCy_3$

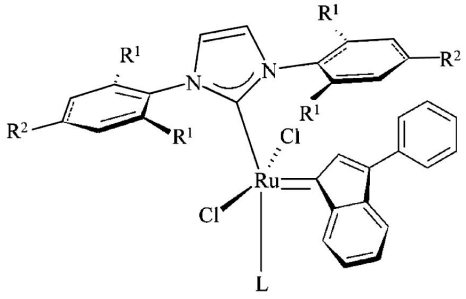


**3a** $R^1$ = Me, $R^2$ = Me, L = $PPh_3$
**3b** $R^1$ = *i*Pr, $R^2$ = H, L = $PPh_3$
**3c** $R^1$ = Me, $R^2$ = Me, L = $PCy_3$
**3d** $R^1$ = *i*Pr, $R^2$ = H, L = $PCy_3$

Scheme 1. First- and second-generation Ru-benzylidene (**1**) and -indenylidene (**2**, **3**) precatalysts.

[a] Department of Inorganic and Physical Chemistry, Ghent University,
Krijgslaan 281 (S3), 9000 Ghent, Belgium
Fax: +-32-9-264-4983
E-mail: francis.verpoort@UGent.be
[b] Institute of Organic Chemistry of the Romanian Academy, Bucharest, Romania

ligands (**5**) and this appealing alternative attracted our attention.[2p] As part of our ongoing research on indenylidene Ru complexes, we here report on the synthesis of five-coordinate ruthenium indenylidene complexes (**5**, **6** and **7**) bearing a saturated N-heterocyclic carbene ligand as viable pre-catalysts, performing efficiently in the RCM of α,ω-dienes and the ROMP of cycloolefins. To determine the activity of this class of indenylidene catalysts relative to the analogous Grubbs' catalysts in classic olefin metathesis reactions, the benzylidene family was used as a benchmark and activities were compared mutually and reciprocally. We believe that such examination is relevant for the understanding of the importance of the carbene unit and the synergetic effect of ancillary ligands around the Ru centre.

## Results and Discussion

While **3c** is readily obtained from **2b** and the free IMes carbene in hot hexane,[2b] an analogous approach is to be avoided in the case of **5**. Because of the comparatively higher air and moisture sensitivity of the unbound saturated carbene, SIMes, an in situ generation protocol is to be used instead. Several known methodologies affording free carbenes[2b,3c–3g,4] led to poor yields in isolated complex **5**. The most suitable method for converting **2b** into its second-generation analogues appeared to be the "one-pot" thermal decomposition of specific adducts[5] such as the chloroform adduct **4** (Scheme 2).

Progress of the reaction was monitored by $^{31}P$ NMR following the increase of a new, upfield peak at $\delta$ = 27.0 ppm, versus $\delta$ = 33.5 ppm for the starting complex **2b**. Complete reaction was observed within 1.5 h and the complex was isolated in excellent yield (82%). In agreement with the proposed structure, NMR spectra showed peaks characteristic for the indenylidene unit [$^1H$ NMR: doublet for $H^8$ at $\delta$ = 9.13 ppm (**5**), vs. $\delta$ = 9.08 ppm in **3c**,[2b] and singlet for $H^2$ at $\delta$ = 7.81 ppm (**5**), vs. $\delta$ = 7.80 ppm in **3c**[2b]] and the imidazolin-2-ylidene ligand ($^1H$ NMR: complex multiplet at $\delta$ = 3.41–3.12 ppm and $^{13}C$ NMR: doublet at $\delta$ = 216.34 ppm for the carbene-C).

Synthesis of **7** proceeded easily by treatment of **5** with an excess of pyridine. However, while for the synthesis of Grubbs' third-generation catalyst **8** the phosphane ligand in **1c** was readily displaced by pyridine (by an associative mechanism[6a]), ligand substitution in the SIMes-indenylidene series proved to be significantly slower, presumably because of: (i) the bulkier indenylidene entity resulting in enhanced steric hindrance around the metal centre and (ii) its stronger electron-donating ability and thus *trans* influence,[7] as compared to the benzylidene ligand, both factors hindering the coordination of pyridine *trans* to the indenylidene moiety. As a consequence, a strongly diminished rate of pyridine complex formation is observed, which is consistent with the low rate of $PCy_3$ ligand dissociation. The indenylidene complex **7** was isolated in good yield (70%) as an orange-brown powder. In contrast to the

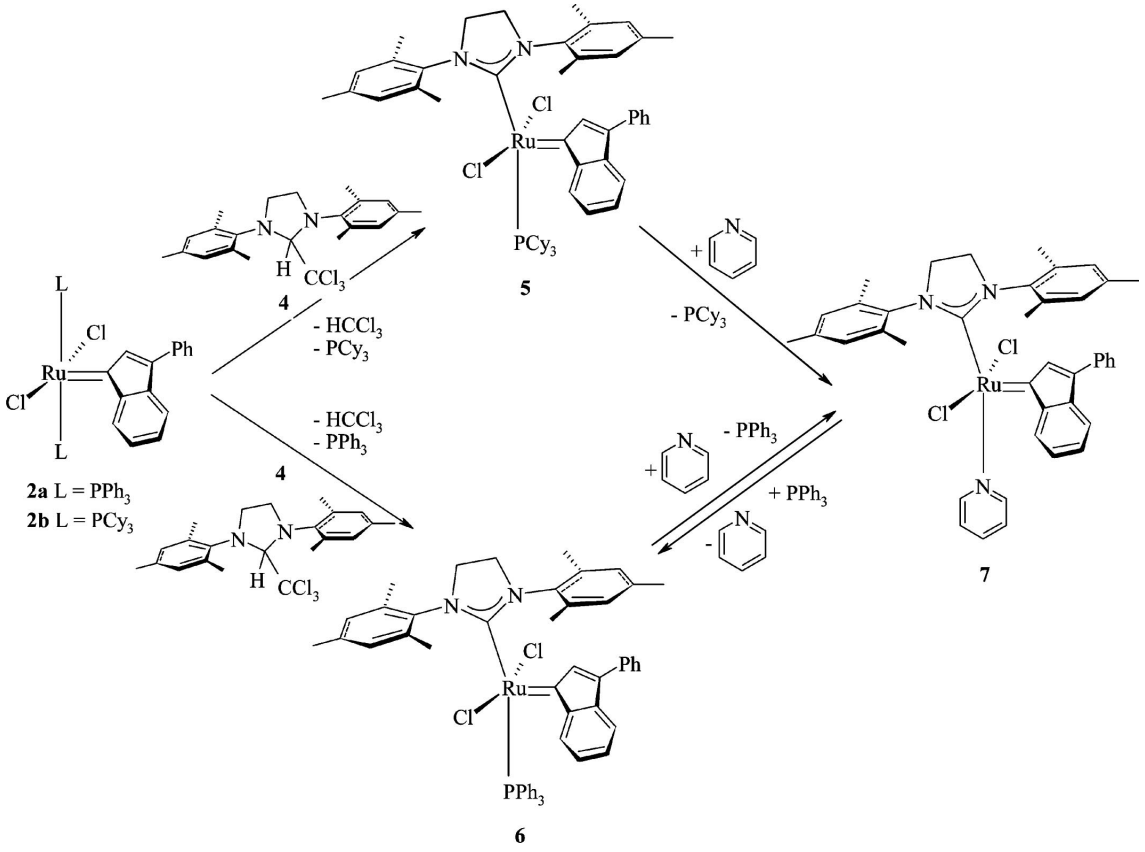


Scheme 2. Synthetic pathways to second- (**5**, **6**) and third-generation indenylidene-Ru (**7**) metathesis catalysts.

  

Grubbs' (**8a**, **9**)[6] and Nolan (**10**)[2l] complexes, which incorporate two pyridine ligands (Scheme 3), the $^1$H and $^{13}$C NMR spectra indicated coordination of only one pyridine. Elemental analysis confirmed this statement indisputably. Unlike **8a**,**b**, complex **7** is stable in dichloromethane (clear red solutions) for several days, at room temperature.

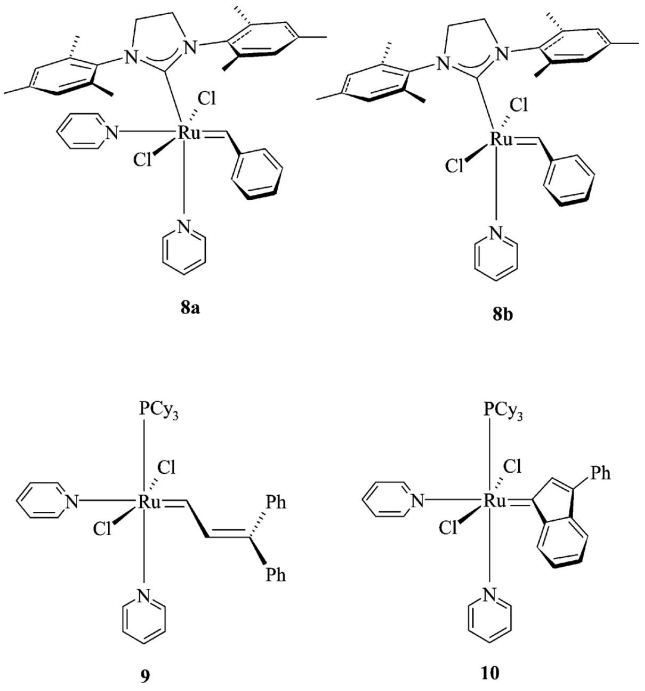


Scheme 3. Pyridine-containing Ru precatalysts.

This enhanced thermal stability is likely a result of the steric and electronic robustness of the indenylidene ligand, which prevents dimerization, the initial step towards catalyst decomposition.[8] This robustness is a unique feature for a third-generation catalyst, while the labile pyridine ligand is an asset for fast initiation in ROM polymerizations.[3i,3j]

## Structure Validation

In order to characterize the compound and to validate the structure of compound **7**, a series of 2D NMR techniques including homonuclear COSY spectroscopy and heteronuclear HSQC and HMBC spectroscopy were used.

The initial analysis of the $^1$H NMR spectra reveals the resonance of $H^8$ at $\delta$ = 9.10 ppm in the indenylidene moiety that is generally well recognizable as it gives rise to the only doublet, as well as six singlets (1.70–2.90 ppm) due to six methyl groups from the SIMes ligand. Low-field quaternary resonances associated with the carbene atoms of the indenylidene (Ru=CR) and NHC moieties, as well as signals of the pyridine ligand, are visible in $^{13}$C NMR spectroscopy. The protons that are directly attached to the carbons of the imidazolidene ring can be deduced from the HSQC spectrum [3.17–3.56 ppm ($^1$H); ca. 50.6, ca. 52.1 ppm ($^{13}$C)]. Correlations can be found between these protons and the carbon atom with high chemical shifts ($\delta$ = 215 ppm, HMBC). The aromatic protons of the SIMes ligand (6.77, 6.60 ppm) could be assigned on the basis of an HMBC correlation with the methyl carbon signals and their mutual correlation by $^1$H–$^1$H COSY (Figure 1). The pyridine protons were distinguished on the basis of the number of observed $^1$H–$^1$H COSY correlations. As a starting point for the analysis of the indenylidene ligand, the quaternary carbene atom was chosen as it will resonate at high frequency. Such a signal is observed in the 1D $^{13}$C spectrum at $\delta$ = 301 ppm. The singlet due to alkylidene carbon correlates with singlets $H^{[2]}$ ($\delta$ = 7.23 ppm) and $H^8$ ($\delta$ = 9.10 ppm) (HMBC). A distinction between those two protons can be made by their multiplicity, as all four resonances are well-resolved. The $^1$H–$^1$H COSY experiment also permitted location of the $H^1$–$H^9$ spin system. HMBC correlations were then used to assign the quaternary carbon atoms in the main aromatic ring system.

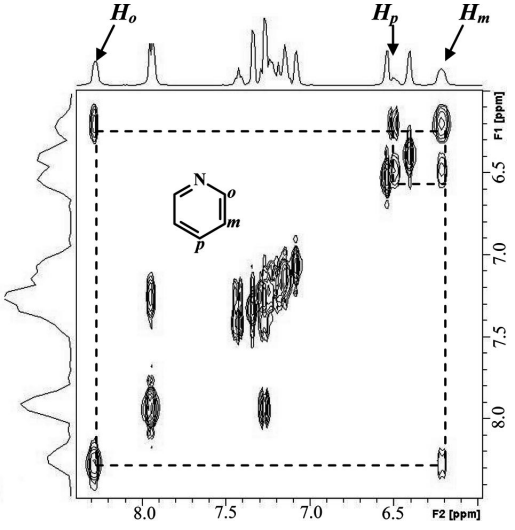


Figure 1. Aromatic section of the $^1$H–$^1$H COSY for complex **7**.

Complex **6** was obtained from **7** by simple ligand exchange and isolated in 89% yield as a clear red powder. In addition, it was straightforwardly obtained from reaction of **2a** with **4** (1 h in refluxing THF). The high thermal stability of **2a** prevents decomposition under these conditions and thus provides a cheap and economical way to obtain this second-generation-type catalyst.

Challenged to establish how the properties of the indenylidene ligand translate into catalyst activity, we investigated the catalytic behaviour of the indenylidene complexes **2b**, **5**, **6** and **7** for two standard reactions, the ROMP of 1,5-cyclooctadiene (COD, **11**) (Scheme 4) and the RCM of diethyl diallylmalonate (**13**) (Scheme 6), usually employed

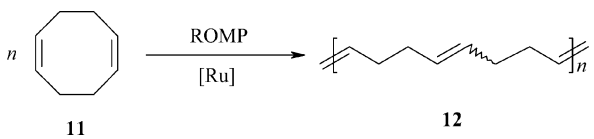


Scheme 4. Ring-opening metathesis polymerization of 1,5-cyclooctadiene (**11**).

  

for the characterization of olefin metathesis catalysts.[9] Parallel screening with their benzylidene counterparts **1a**, **1c** and **8b** has been performed to gain insight into particularities concerning the carbene ligand behaviour.

In the ROMP of 3000 equiv. COD, catalyst **5** suffers from a strongly increased initiation period in comparison with its benzylidene analogue, **1c** (Figure 2). Still, full conversion is achieved after 5 h, which again illustrates the stability of the precursor. The lower rate of initiation of **5** relative to **1c** is in accordance with what was observed in RCM reactions. The replacement of the $PCy_3$ ligand (**5**) with the more labile $PPh_3$ ligand (**6**) rationally enhances the initiation rate and drastically improves monomer consumption, reaching full conversion within a few minutes.

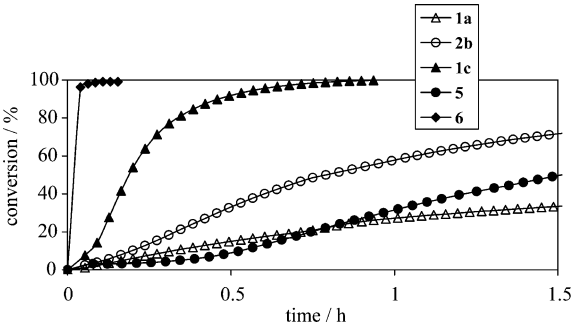


Figure 2. ROMP of 3000 equiv. COD (**11**) using catalysts **1a**, **1c**, **2b**, **5** and **6**. Catalyst concentration: 0.453 mM; solvent: $CDCl_3$; temperature: 20 °C; conversion determined by $^1H$ NMR spectroscopy. Lines are intended as visual aids, not as curve fits.

For the first-generation catalysts, we encountered a strikingly better activity for catalyst **2b** versus **1a**. As the propagating species is the same for both catalysts, a fundamental difference has to be native to the precatalysts. Surprisingly, at a monomer/catalyst ratio of only 300 (Figure 3), the benzylidene catalyst demonstrates superior activity compared with the indenylidene analogue, which is at first sight opposite to the previously discussed results.

In fact, catalyst **2b** displays an initiation period after which activity increases to reach 97% conversion after 1 h. Contrary to the observations, the bulkier indenylidene unit would predict faster $PCy_3$ ligand dissociation as a result of steric repulsion between the carbene unit and the phosphane ligand (Scheme 5, a).[10] On the other hand, it is reasonable to accept that the activation energy for olefin coordination is higher for **2b** than for **1a** because of: (i) the enhanced steric hindrance of the indenylidene ligand, preventing facile approach of olefin substrate molecules (Scheme 5, b), (ii) the better electron-donating properties of the indenylidene ligand, saturating the Ru centre and thus decreasing the electron affinity at the active site (Scheme 5, b) and (iii) the better delocalization of electron density in the indenylidene ligand relative to the benzylidene ligand, which reduces the rate of metallacyclobutane ring formation (Scheme 5, c). These arguments account for the prolonged initiation period of **2b** and illustrate how olefin coordination, the second step of the initiation process, can play a determining role in the initiation rate of the catalyst and accordingly demonstrates the importance of the steric and electronic characteristics of the carbene unit. The faster initiation of the benzylidene catalyst, **1a**, affords higher concentrations of the active species and consequently more catalyst decomposes by bimolecular decomposition.

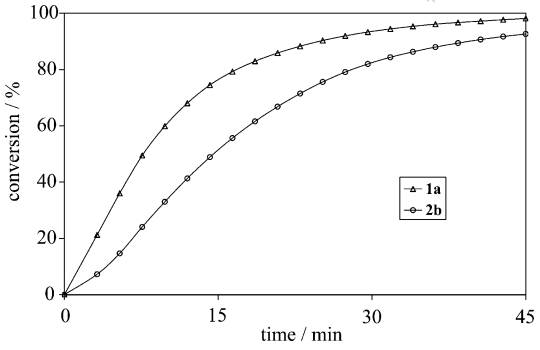


Figure 3. ROMP of 300 equiv. COD (**11**) using catalysts **1a** and **2b**. Catalyst concentration: 4.53 mM; solvent: $CDCl_3$; temperature: 20 °C; conversion determined by $^1H$ NMR spectroscopy. Lines are intended as visual aids, not as curve fits.

For the third-generation catalysts, the monomer/catalyst ratio was extended to 10000:1 and the results are depicted in Figure 3.

Quite successfully, at these low catalyst loadings, **7** reached full monomer conversion in less than 15 min, surpassing at all times the third-generation Grubbs' catalyst **8b** (Figure 4), the ROMP catalyst of excellence until now. The polymers obtained from these reactions display similar characteristics ($M_n$ = 52000; PDI = 1.6; $\sigma_c$ = 0.47 for **8b** and $M_n$ = 50000; PDI = 1.6; $\sigma_c$ = 0.42 for **7**).

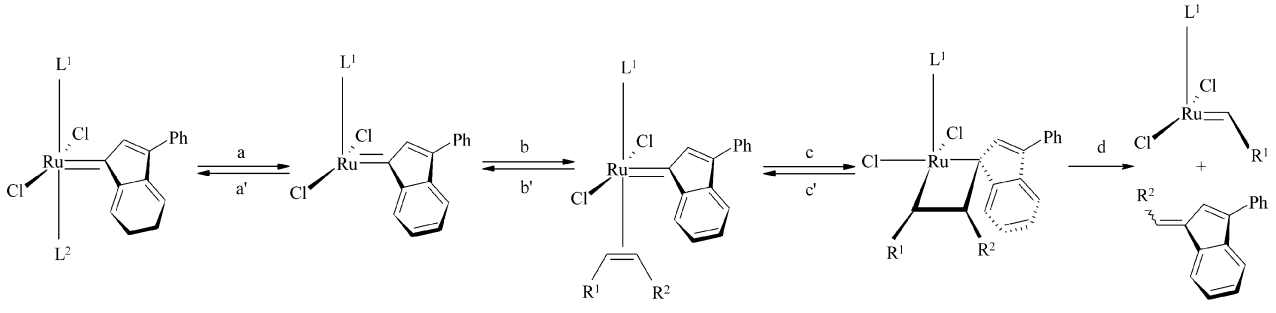


Scheme 5. Mechanism of initiation for indenylidene-type precatalysts.

  

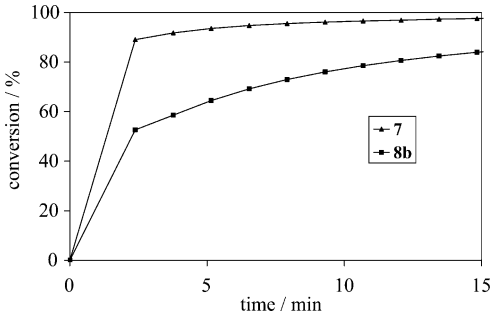


Figure 4. ROMP of 10000 equiv. COD using third-generation catalysts Ru-indenylidene, **7**, versus Ru-benzylidene, **8b**. Catalyst concentration: 0.136 mM; temperature: 20 °C; solvent: $CDCl_3$; conversion determined by $^1H$ NMR spectroscopy. Lines are intended as visual aids, not as curve fits.

Summarizing the results for ROMP, the electronic and steric robustness of the indenylidene ligand raises the barrier for catalyst initiation and decomposition. The lower initiation rate is particularly disadvantageous in view of 'living' polymerizations with catalysts **2b** and **5**, while the enhanced stability is beneficial for complexes **6** and **7**.

Aiming at a more elaborate exploration of the catalytic potential of the newly reported complexes and encouraged by the high rates of initiation for complex **7**, our research was extended to the application in the RCM of diethyl diallylmalonate, **13** (Scheme 6).

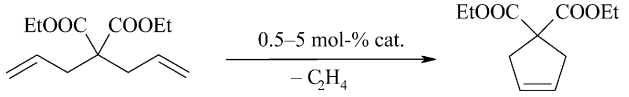


**13** **14**

Scheme 6. Ring-closing metathesis of diethyl diallylmalonate (**13**).

The results for the RCM of **13** using catalysts **1a**, **1c**, **2b**, **5** and **6** are depicted in Figure 5. Remarkably, under these conditions, first-generation catalysts **1a** and **2b** clearly afford higher conversions in shorter reaction times than their second-generation counterparts, **1c** and **5**, which obviously originates from an increased ligand dissociation.[3j] Within the class of first-generation catalysts, the indenylidene catalyst performs a faster quantitative consumption of the substrate. Both catalysts show high initial activity followed by a slow phase proceeding towards full conversion, a highly unusual reaction profile also described by Grubbs et al. for **1a**.[9]

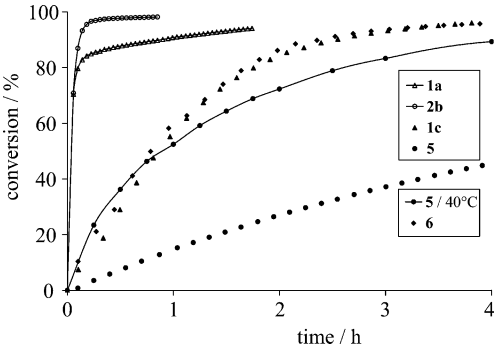


Figure 5. Conversions in the RCM of diethyl diallylmalonate (**13**) using catalysts **1a**, **1c**, **2b**, **5** and **6**. Catalyst loading: 0.5 mol-%; temperature: 20 °C; solvent: $CDCl_3$; conversion determined by $^1H$ NMR spectroscopy. Lines are intended as visual aids, not as curve fits.

We believe that a decreased rate of initiation for the indenylidene catalyst relative to the benzylidene catalyst affords lower concentrations of the active species and, as a result, less decomposition occurs.[8] Therefore, higher conversions are possible for the slower initiating catalyst **2b** than for **1a**.

Using a low catalyst loading of 0.5 mol-%, precursor **5** shows only 45% conversion in the RCM of **11** after 4 h, a result which is clearly excelled by the Grubbs' second-generation catalyst **1c**. A further increase of conversion to 76% after 16 h and 90% after 24 h indicates that the catalyst has a very long lifetime; yet, at room temperature a low rate of initiation prevents a fast conversion. The reaction rate speeds up when the temperature is raised to 40 °C. The higher temperature allows for a better ligand dissociation, and hence a higher initiation rate of **5**. Whereas the indenylidene unit in **2b** proved beneficial, incorporation of the NHC ligand decreased the catalytic activity for RCM dramatically. In search of better ligand dissociation, the exchange of the $PCy_3$ ligand in **5** for the more labile $PPh_3$ ligand logically improves the rate of reaction. Remarkably, the activity of **6** is identical to that of **1c**. In spite of the more labile $PPh_3$ ligand, allowing for better ligand dissociation, the activity of **6** does not surpass the activity of **1c**. While **6** clearly initiates faster in the ROMP of **11**, its activity is equal to that of **1c** in the RCM of **13**.

To clarify the behaviour of the third-generation catalysts in RCM, both catalysts have been tested at various catalyst loadings (0.5–5 mol-%) and compared mutually (Figures 6 and 7).

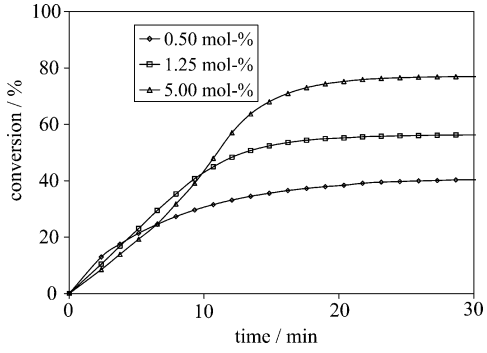


Figure 6. Conversions in the RCM of diethyl diallylmalonate (**13**) using catalyst **8b** at different catalyst loadings. Substrate loading: 0.41 mmol diethyl diallylmalonate; temperature: 20 °C; solvent: 0.60 mL of $CDCl_3$; conversion determined by $^1H$ NMR spectroscopy. Lines are intended as visual aids, not as curve fits.

While the previously discussed catalysts (Figure 4) tend to perform the reaction to full conversion, catalysts **7** and **8b** complete the reaction only partially (Figures 6 and 7). The weak donating properties of the pyridine ligand in complexes **7** and **8b** are visibly insufficient to stabilize the catalytically active species during the course of the reaction,

  

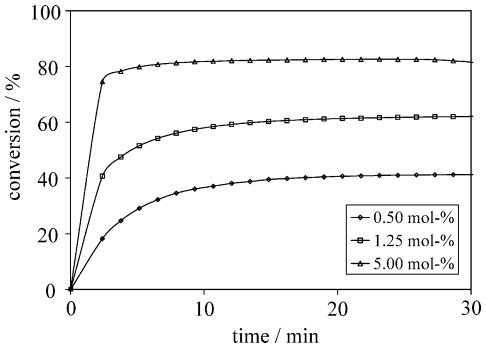


Figure 7. Conversions in the RCM of diethyl diallylmalonate (**13**) using catalyst **7** at different catalyst loadings. Substrate loading: 0.41 mmol diethyl diallylmalonate; temperature: 20 °C; solvent: 0.60 mL of $CDCl_3$; conversion determined by $^1H$ NMR spectroscopy. Lines are intended as visual aids, not as curve fits.

and as a result, catalyst decomposition prevents a successful fulfilment of the reaction. Similar reaction profiles are reported for analogous pyridine-containing complexes **9** and **10**.[2l,6b]

Results further illustrate that, for all tested catalyst loadings, the indenylidene catalyst **7** enables very good conversions at short reaction times (5–10 min), undoubtedly superior to those attained with the benzylidene analogue **8b**. Contrary to the first- and second-generation catalysts, this indenylidene catalyst initiates faster than its benzylidene analogue. Astoundingly, at distinct catalyst loadings, there is no significant differentiation in conversions after longer reaction times (>20 min) between the catalysts mutually. This indicates an unusual catalyst behaviour in the initial stage of the reaction. It is even more conspicuous that in the beginning of the reactions with catalyst **8b**, conversions are lower in the case of higher catalyst loadings. To gain insight into this, the TON/s of both catalysts were analysed in detail (Figures 8 and 9).

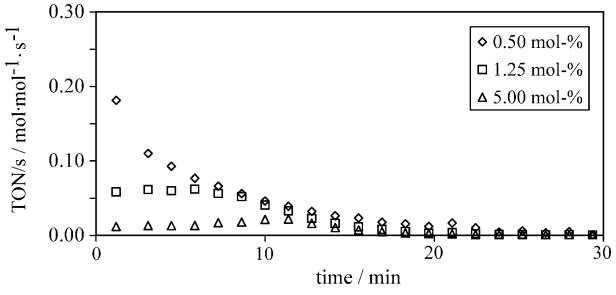


Figure 8. TON/s in RCM of diethyl diallylmalonate (**13**) using catalyst **8b** at different catalyst loadings. Temperature: 20 °C; solvent: $CDCl_3$.

Whereas **7** shows an expected TON/s plot for all catalyst loadings, **8b** demonstrates an initiation period which lengthens with increasing catalyst loadings. This type of behaviour is a fingerprint of intermolecular self-inhibition of the catalyst, while the overall conversion, being roughly equal for both catalysts, excludes major decomposition of the starting complex in this stage of the reaction. NMR investigation of this event revealed the ascent of a new signal at $\delta$ = 8.84 ppm in the $^1H$ NMR spectrum (pyridine-*o*-C*H*) and two distinct peaks at $\delta$ = 152.3 ppm and $\delta$ = 150.1 ppm in the $^{13}C$ NMR spectrum (pyridine-*o*-*C*) (Figure 10), unambiguously characterizing the formation of the bispyridine complex, **8a**.[6a]

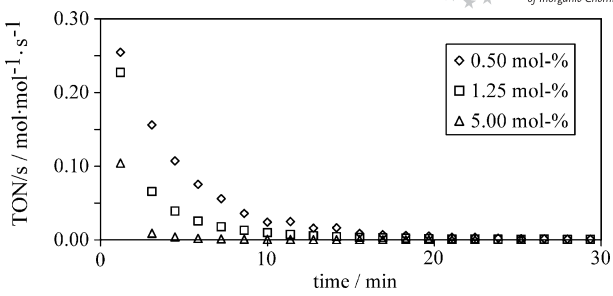


Figure 9. TON/s in RCM of diethyl diallylmalonate (**13**) using catalyst **7** at different catalyst loadings. Temperature: 20 °C; solvent: $CDCl_3$.

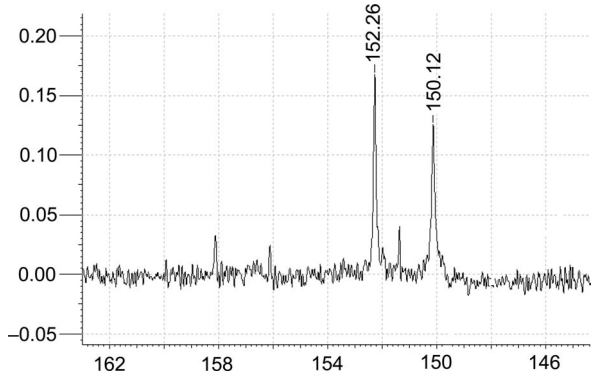


Figure 10. Detail of the $^{13}C$ NMR spectrum of **8b** at room temperature. Solvent: $CDCl_3$, concentration: 34.5 mM.

Based on these observations, we propose a mechanism where the starting compound **8b** partially disproportionates into a bispyridine complex and a proposed unidentified dimeric species.[11] We previously emphasized the steric and electronic robustness of the indenylidene unit, which disfavours dimerization and decomposition of the precatalyst. It is conceivable that, because of enhanced steric crowding of the indenylidene ligand, the driving force for the formation of a dimeric species and a bispyridine complex has decreased to such an extent that this phenomenon does not occur spontaneously and as a result, the catalyst displays a different behaviour in the initial phase of the reaction. As the propagating species are identical for both catalyst precursors, and thus are equally vulnerable to decomposition, conversions are similar in the end. In search of further support of this statement, we reasoned that if the bispyridine complex formation accounts for the observed initiation periods, such an initiation period should be absent in the case of the bispyridine catalyst **8a**. Figures 11 and 12 show that indeed the bispyridine complex exhibits no visible initiation period.

  

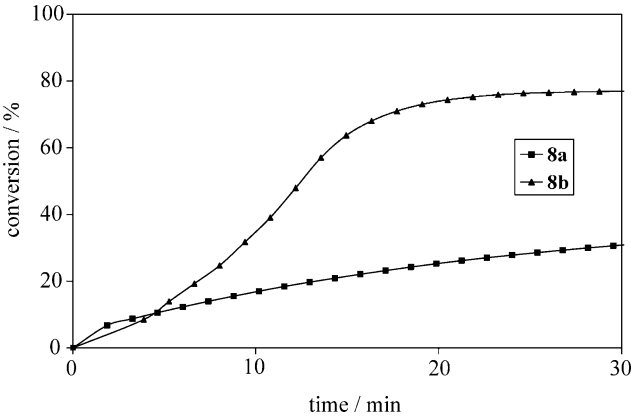


Figure 11. Conversions in RCM of diethyl diallylmalonate (**13**) using catalysts **8a** and **8b**. Catalyst loading: 5 mol-%; temperature: 20 °C; solvent: $CDCl_3$; conversion determined by $^1H$ NMR spectroscopy. Lines are intended as visual aids, not as curve fits.

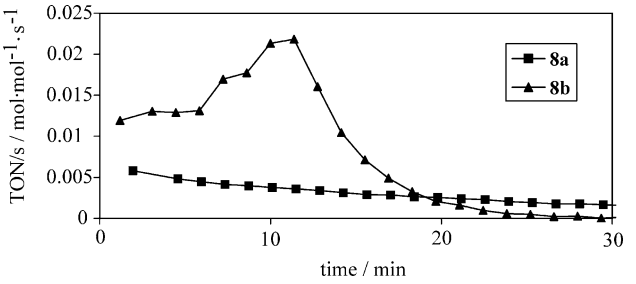


Figure 12. TON/s in RCM of diethyl diallylmalonate (**13**) using catalysts **8a** and **8b**. Catalyst loading: 5 mol-%; temperature: 20 °C; solvent: $CDCl_3$. Lines are intended as visual aids, not as curve fits.

In summary, in first- and second-generation catalysts the indenylidene unit evokes a decreased initiation rate in the RCM reaction, still allowing for full conversions. In the case of third-generation catalysts, the indenylidene unit stabilizes the precatalyst and prevents it from self-inhibition.

## Conclusions

In conclusion, in this work new and robust second- and third-generation Ru-indenylidene complexes **5**, **6** and **7**, all isolated in high yields, have been disclosed as air- and moisture-stable compounds. Together with the first-generation catalyst, this family of Ru-indenylidenes was screened for their activity for RCM and ROMP of model substrates, with their benzylidene counterparts as benchmarks. Based on kinetic investigations, the alkylidene ligand was shown to play a decisive role in the activity of the catalysts. More specifically, a decreased rate of catalyst initiation for the indenylidene complexes was observed. For first-generation catalysts, the retarded initiation of the indenylidene catalyst affords higher activity in RCM, while the activity in ROMP is more dependent on the reaction conditions. The second-generation indenylidene catalyst **5** exhibits lower activity than its benzylidene analogue, in RCM reactions as well as in ROM polymerizations; clearly a result of decreased catalyst initiation. While catalyst **6** shares the activity of the second-generation Grubbs' catalyst for RCM, it initiates ROMP significantly faster. Evaluating the results for the third-generation catalysts, we observed a better performance of the indenylidene catalyst **7** both in RCM and ROMP. The higher activity and stability of **7** versus **8b** supports the idea that properties such as catalyst activity and stability, seemingly antagonistic, can be innate features of one single catalyst. Serendipitously, determining the activity of **8b** for RCM at different catalyst loadings revealed the unexpected partial formation of the bispyridine complex **8a** from **8b**, which results in the self-inhibition of the catalyst.

## Experimental Section

**General Remarks:** All synthetic manipulations were performed under argon (oxygen-free) using the Schlenk technique. Argon was dried by passage through Drierite. Tetrahydrofuran (THF), toluene, dichloromethane, hexane, [$D_6$]benzene and [D]chloroform, dried by standard methods, were degassed by the standard three freeze-pump-thaw cycles. Methanol and pyridine were not dried or degassed before use. $PPh_3$ was purchased from Acros. Catalysts **1c**[3e] and **8b**[6a] were prepared according to the literature. Catalyst **1a** and diethyl diallylmalonate were purchased from Aldrich and used as received. Catalyst **2b** was supplied by Umicor AG and used as received. 1,5-Cyclooctadiene was purchased from Aldrich and distilled, dried and degassed before use. $^1H$ NMR spectra were recorded with a Bruker Avance 500 MHz spectrometer and $^{13}C$ and $^{31}P$ NMR spectra were recorded with a Bruker 300 MHz spectrometer. Chemical shifts ($\delta$) are given in parts per million (ppm) relative to TMS. In $^{31}P$ NMR spectra, $PPh_3$ was used as an internal standard ($\delta$ = –4.27 ppm in $C_6D_6$). Kinetic experiments were conducted on a Varian Unity 300-MHz NMR spectrometer.

**Abbreviations:** NHC = N-heterocyclic carbene; RCM = ring-closing metathesis; ROMP = ring-opening metathesis polymerization; Cy = cyclohexyl; Ph = phenyl; py = pyridine; SIMes = *N*,*N*′-bis(2,4,6-trimethylphenyl)imidazolin-2-ylidene; IMes = *N*,*N*′-bis(2,4,6-trimethylphenyl)imidazol-2-ylidene; IPr = *N*,*N*′-bis(2,6-diisopropylphenyl)imidazolin-2-ylidene; TON = turn over number.

**Synthesis of (SIMes)($PCy_3$)$Cl_2$Ru(3-phenylinden-1-ylidene) (5):** Complex **2b** (398 mg, 0.432 mmol) and the chloroform adduct **4** (357 mg, 0.863 mmol) were admitted into a previously flame-dried flask and solved in THF (15 mL) whilst stirring, and the solution was refluxed for 1.5 h. The reaction mixture was cooled down, solid materials were filtered off and the filtrate was concentrated in vacuo. The residue was suspended in MeOH (5 mL) and dissolved under ultrasound; the precipitate formed when the ultrasound was disconnected, was filtered off, washed on the funnel with another 5 mL of MeOH and dried in vacuo to afford **5** (334.5 mg, 82% yield) as a red powder. $^1H$ NMR (500.13 MHz, 22 °C, $C_6D_6$, $Me_4Si$): $\delta$ = 9.13 (d, $J_{8,7}$ = 7.3 Hz, 1 H, $H^8$), 7.88 (s, 1 H, phenyl), 7.86 (s, 1 H, phenyl), 7.81 (s, 1 H, $H^2$), 7.31 (t, $J_\alpha$ = 7.4 Hz, 1 H, phenyl), 7.23 (t, $J_\alpha$ = 7.5 Hz, 2 H, phenyl), 7.16 (td, $J_{8,7}$ = $J_{7,6}$ = 7.3, $J_{7,5}$ = 1.2 Hz, 1 H, $H^7$), 7.10 (td, $J_{7,6}$ = $J_{6,5}$ = 7.2, $J_{6,8}$ = 1.0 Hz, 1 H, $H^6$), 7.06 (dd, $J_{6,5}$ = 7.2, $J_{7,5}$ = 1.2 Hz, 1 H, $H^5$), 6.96 (s, 1 H, SIMes-*m*-C*H*), 6.95 (s, 1 H, SIMes-*m*-C*H*), 6.45 (s, 1 H, SIMes-*m*-C*H*), 6.00 (s, 1 H, SIMes-*m*-C*H*), 3.41–3.32 (m, 2 H, N-C*H*), 3.28–3.22 (m, 1 H, N-C*H*), 3.18–3.12 (m, 1 H, N-C*H*), 2.85 (s, 3 H, SIMes-C$H_3$), 2.83 (s, 3 H, SIMes-C$H_3$), 2.45 (q, $J_\alpha$ = 11.5 Hz, 3 H, $PCy_3$), 2.36 (s, 3 H, SIMes-C$H_3$), 2.22 (s, 3 H, SIMes-C$H_3$), 2.21 (s, 3 H, SIMes-C$H_3$), 1.82 (m, 3 H, $PCy_3$), 1.78 (s, 3 H, SIMes-C$H_3$), 1.71 (m, 3 H, $PCy_3$), 1.57 (m, 3 H, $PCy_3$), 1.52 (m, 6 H,

  

$PCy_3$), 1.36–1.09 (m, 15 H, $PCy_3$) ppm. $^{13}C$ NMR (300.18 MHz, 22 °C, $C_6D_6$, $Me_4Si$): $\delta$ = 291.4 (d, $J_{P-C}$ = 2 Hz, 1 C, $C^1$), 216.3 (d, $J_{P-C}$ = 292 Hz, 1 C, SIMes-$C^2$), 144.1, 140.1, 138.1, 136.9, 136.9, 136.4, 136.1, 135.6, 135.2, 134.7, 129.0, 128.9, 128.44, 128.04, 127.95, 127.6, 127.4, 127.0, 126.6, 126.3, 125.8, 125.3, 115.0, 51.1, 50.5, 32.1, 31.9, 30.3, 28.8, 28.5, 26.9, 26.8, 26.7, 25.8, 25.3, 21.6, 19.8, 19.7, 19.3, 17.8, 17.6 ppm. $^{31}P$ NMR (300.18 MHz, 22 °C, $C_6D_6$): $\delta$ = 27.0 (s) ppm. $C_{54}H_{69}Cl_2N_2PRu$ (949.10): calcd. C 68.34, H 7.33, N 2.95; found C 67.97, H 6.95, N 3.19.

**Synthesis of (SIMes)($PPh_3$)$Cl_2$Ru(3-phenylinden-1-ylidene) (6). Method A:** Complex **7** (1.00 g, 1.34 mmol) and $PPh_3$ (387 mg, 1.47 mmol) were dissolved in dichloromethane (50 mL) and stirred for 30 min at room temperature. The solvent was removed by evaporation and the residue recrystallized from dichloromethane/hexane. Filtration and washing with hexane afforded compound **6** (1.11 g, 89%).

**Method B:** Complex **2a** (1.00 g, 1.13 mmol) and the chloroform adduct **4** (935 mg, 2.26 mmol) were charged into a flame-dried reaction flask and dissolved in toluene (50 mL). The mixture was heated for 2.5 h at 65 °C. After cooling down to room temperature, the solid materials were filtered off and the filtrate was concentrated by evaporation. Suspending in hexane, filtering off and washing intensively with hexane (100 mL) yielded compound **6** as a deep red powder in 86% yield.

$^1H$ NMR (300.18 MHz, 22 °C, $CD_2Cl_2$, $Me_4Si$): $\delta$ = 7.87 (d, $J$ = 7.7 Hz, 1 H, $H^8$), 7.54–6.96 (br. multiple peaks, 20 H, $PPh_3$, phenyl, $H^2$, $H^5$, $H^6$, $H^7$, SIMes-*m*-C*H*), 6.56 (s, 1 H, SIMes-*m*-C*H*), 6.41 (s, 1 H, SIMes-*m*-C*H*), 6.03 (s, 1 H, SIMes-*m*-C*H*), 4.09–4.03 (m, 2 H, N-C*H*), 3.89–3.78 (m, 2 H, *N*-C*H*), 2.69 (s, 3 H, SIMes-C$H_3$), 2.66 (s, 3 H, SIMes-C$H_3$), 2.47 (s, 3 H, SIMes-C$H_3$), 2.13 (s, 3 H, SIMes-C$H_3$), 2.01 (s, 3 H, SIMes-C$H_3$), 1.84 (s, 3 H, SIMes-C$H_3$) ppm. $^{13}C$ NMR (300.18 MHz, 22 °C, $CD_2Cl_2$, $Me_4Si$): $\delta$ = 300.3 (d, $J_{P-C}$ = 13 Hz, 1 C, $C^1$), 215.2 (d, $J_{P-C}$ = 78 Hz, 1 C, SIMes-$C^2$), 143.3, 141.2, 140.8, 139.6, 139.4, 138.6, 138.2, 137.2, 136.9, 136.8, 136.4, 135.8, 134.8, 134.5, 134.4, 134.0, 133.7, 132.2, 132.0, 131.5, 130.1, 130.0, 129.9, 129.5, 129.2, 129.1, 129.0, 128.93, 128.86, 128.7, 128.2, 127.6, 127.5, 127.3, 126.6, 116.4, 21.3, 20.9, 20.4, 20.3, 18.7, 18.6 ppm. $^{31}P$ NMR (300.18 MHz, 22 °C, $CD_2Cl_2$): $\delta$ = 27.3 (s) ppm. $C_{54}H_{51}Cl_2N_2PRu$ (930.96): calcd. C 69.67, H 5.52, N 3.01; found C 69.78, H 5.43, N 3.19.

**Synthesis of (SIMes)(py)$Cl_2$Ru(3-phenylinden-1-ylidene) (7):** A flame-dried reaction flask was charged with **5** (1.00 g, 1.05 mmol) and pyridine (5.0 mL). The resulting solution was stirred for 2 h, during which time the colour changed from red to yellowish-brown. Hexane (20 mL) was added and upon cooling the mixture to –40 °C, a brown solid precipitated. The solid was filtered, washed several times with cold hexanes (3 × 10 mL) and dried under vacuum to afford **7** as an orange-brown solid. Yield: 552 mg (70%). $^1H$ NMR (300.18 MHz, 22 °C, $C_6D_6$, $Me_4Si$): $\delta$ = 9.05 (d, 1 H, $H^8$), 8.13 (br. s, 2 H, py-*o*-C*H*), 7.81–6.04 (br. multiple peaks, 16 H, py, $H^5$, $H^6$, $H^7$, Mes-C*H*), 3.56–3.17 (m, 4 H, N-C$H_2$), 2.99 (s, 3 H, SIMes-C$H_3$), 2.72 (s, 3 H, SIMes-C$H_3$), 2.48 (s, 3 H, SIMes-C$H_3$), 2.13 (s, 3 H, SIMes-C$H_3$), 1.99 (s, 3 H, SIMes-C$H_3$), 1.70 (s, 3 H, SIMes-C$H_3$) ppm. $^{13}C$ NMR (300.18 MHz, 22 °C, $C_6D_6$, $Me_4Si$): $\delta$ = 300.6 (s, 1 C, $C^1$), 215.13 (s, 1 C, SIMes-$C^2$), 152.2 (s, 2 C, py-*o*-*C*), 143.6, 141.5, 141.0, 140.6, 139.5, 139.3, 138.8, 137.6, 137.4, 137.2, 137.1, 136.6, 136.2, 134.2, 134.6, 129.8, 129.5, 129.2, 128.6, 128.2, 127.9, 127.6, 126.6, 123.2, 116.8, 52.1, 50.6, 21.5, 21.2, 21.04, 20.95, 18.8, 18.6 ppm. $C_{41}H_{41}Cl_2N_3Ru$ (747.77): calcd. C 65.68, H 5.53, N 5.62; found C 65.22, H 5.87, N 5.43. For numbering of the indenylidene ring system see Figure 13.

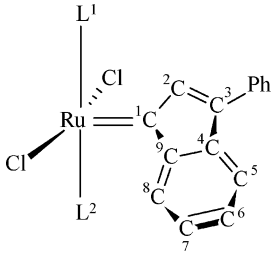


Figure 13. Numbering of the indenylidene ring system.

**General Procedure for Ring-Closing Metathesis:** The appropriate amount of catalyst was dissolved in $CDCl_3$ (0.60 mL), left to equilibrate for 2 min at room temperature and transferred to an NMR tube. Diethyl diallylmalonate (0.10 mL, 0.41 mmol) was then added under argon and the NMR tube capped and sealed with Parafilm. Conversion was monitored by integration of the allylic methylene peaks in the $^1H$ NMR spectrum of the substrate and the product.

**General Procedure for Ring-Opening Metathesis Polymerization:** The appropriate amount of catalyst was dissolved in $CDCl_3$ (0.60 mL) and transferred to an NMR tube. 1,5-Cyclooctadiene (0.10 mL, 0.82 mmol) was then added under argon and the NMR tube was capped. Conversion was monitored by integration of the allylic methylene peaks in the $^1H$ NMR spectrum of the monomer and polymer.

**General Procedure for Polymer Synthesis:** A small oven-dried glass vial with septum was charged with a magnetic stir bar and the appropriate amount of catalyst was added under inert argon. The catalyst was dissolved (5.0 mL of $CH_2Cl_2$) and COD (2.0 mL) was transferred to the vial by syringe, under vigorous stirring at room temperature. The polymerization was terminated after 1 h through addition of ethyl vinyl ether (0.1 mL) and a small amount of BHT was added to prevent the polymer from oxidation. The polymer was precipitated with methanol and isolated by filtration and drying in vacuo. $M_n$ and polydispersities (PDI) were determined by size-exclusion chromatography (SEC) with polystyrene calibration. $\sigma_c$ was determined by $^{13}C$ NMR spectroscopy (allylic carbon *cis*: $\delta$ = 27.6 ppm, allylic carbon *trans*: $\delta$ = 32.9 ppm).

**NMR Investigation on Catalyst 8b:** An NMR tube was charged with a solution of **8b** (34.5 mM) in $CDCl_3$ under inert argon and the NMR tube was capped and sealed with Parafilm. The catalyst transformation was monitored at room temperature by $^1H$ and $^{13}C$ NMR spectroscopy.

## Acknowledgments

S. M. is indebted to the Institute for the Promotion of Innovation through Science and Technology in Flanders (IWT Flanders) and Research fund of Ghent University for a research grant. F. V. is grateful to the FWO Flanders (Fund for Scientific Research-Flanders) for financial support. Umicore AG is acknowledged for a generous gift of compound **2b**. We are thankful to J. Martins of Ghent University for NMR measurements and to Olivier F. Grenelle and Dr. Marc G. Proot of Chevron Technology, Ghent, for elemental analysis.

[1] For selected reviews on olefin metathesis, see: a) R. H. Grubbs (Ed.), *Handbook of Metathesis*, Wiley-VCH, Weinheim, **2003**; b) A. Fürstner, *Angew. Chem. Int. Ed.* **2000**, *39*, 3013–3043; c) R. R. Schrock, A. H. Hoveyda, *Angew. Chem. Int. Ed.* **2003**,

  

*42*, 4592–4633; d) R. H. Grubbs, *Tetrahedron* **2004**, *60*, 7117–7140; e) D. Astruc, *New J. Chem.* **2005**, *29*, 42–56.

[2] a) H.-J. Schanz, L. Jafarpour, E. D. Stevens, S. P. Nolan, *Organometallics* **1999**, *18*, 5187–5190; b) L. Jafarpour, H.-J. Schanz, E. D. Stevens, S. P. Nolan, *Organometallics* **1999**, *18*, 5416–5419; c) A. Fürstner, A. F. Hill, M. Liebl, J. D. E. T. Wilton-Ely, *Chem. Commun.* **1999**, 601–602; d) A. Fürstner, O. R. Thiel, L. Ackermann, H.-J. Schanz, S. P. Nolan, *J. Org. Chem.* **2000**, *65*, 2204–2207; e) A. Fürstner, O. Guth, A. Düffels, G. Seidel, M. Liebl, B. Gabor, R. Myonott, *Chem. Eur. J.* **2001**, *7*, 4811–4820; f) T. Opstal, F. Verpoort, *Synlett* **2002**, 935–941; g) T. Opstal, F. Verpoort, *Angew. Chem. Int. Ed.* **2003**, *42*, 2876–2879; h) R. Castarlenas, P. H. Dixneuf, *Angew. Chem. Int. Ed.* **2003**, *42*, 4524–4527; i) V. Dragutan, I. Dragutan, F. Verpoort, *Platinum Met. Rev.* **2005**, *49*, 33–40; j) R. Castarlenas, C. Vovard, C. Fischmeister, P. H. Dixneuf, *J. Am. Chem. Soc.* **2006**, *128*, 4079–4089; k) G. S. Forman, R. M. Bellabarba, R. P. Tooze, A. M. Z. Slawin, R. Karch, R. Winde, *J. Organomet. Chem.* **2006**, *691*, 5513–5516; l) H. Clavier, J. L. Petersen, S. P. Nolan, *J. Organomet. Chem.* **2006**, *691*, 5444–5447; m) R. Drozdzak, B. Allaert, N. Ledoux, I. Dragutan, V. Dragutan, F. Verpoort, *Coord. Chem. Rev.* **2004**, *249*, 3055–3074; n) R. Drozdzak, B. Allaert, N. Ledoux, I. Dragutan, V. Dragutan, F. Verpoort, *Adv. Synth. Catal.* **2005**, *347*, 1721–1743; o) R. Drozdzak, N. Ledoux, B. Allaert, I. Dragutan, V. Dragutan, F. Verpoort, *Cent. Eur. J. Chem.* **2005**, *3*, 404–416; p) During the preparation of this manuscript, Nolan reported on the activity of **5** in RCM: H. Clavier, S. P. Nolan, *Chem. Eur. J.* **2007**, *13*, 8029–8036.

[3] a) P. Schwab, M. B. France, J. W. Ziller, R. H. Grubbs, *Angew. Chem. Int. Ed. Engl.* **1995**, *34*, 2039–2041; b) P. Schwab, R. H. Grubbs, J. W. Ziller, *J. Am. Chem. Soc.* **1996**, *118*, 100–110; c) S. P. Nolan, J. Huang, E. D. Stevens, J. L. Petersen, *J. Am. Chem. Soc.* **1999**, *121*, 2674–2678; d) T. Westkamp, F. J. Kohl, W. Hieringer, D. Gleich, W. A. Herrmann, *Angew. Chem. Int. Ed.* **1999**, *38*, 2416–2419; e) M. Scholl, S. Ding, C. W. Lee, R. H. Grubbs, *Org. Lett.* **1999**, *1*, 953–956; f) M. Scholl, T. M. Trnka, J. P. Morgan, R. H. Grubbs, *Tetrahedron Lett.* **1999**, *40*, 2247–2250; g) J. Huang, H.-J. Schanz, E. D. Stevens, S. P. Nolan, *Organometallics* **1999**, *18*, 5375–5380; h) J. A. Love, J. P. Morgan, T. M. Trnka, R. H. Grubbs, *Angew. Chem. Int. Ed.* **2002**, *41*, 4035–4037; i) T.-L. Choi, R. H. Grubbs, *Angew. Chem. Int. Ed.* **2003**, *42*, 1743–1746; j) J. A. Love, M. S. Sanford, M. W. Day, R. H. Grubbs, *J. Am. Chem. Soc.* **2003**, *125*, 10103–10109. For books on N-heterocyclic carbenes: k) S. P. Nolan (Ed.), *N-Heterocyclic Carbenes in Synthesis*, Wiley-VCH, Weinheim, **2006**; l) F. Glorius, *N-Heterocyclic Carbenes (Nhc) in Transition Metal Catalysis: 21 (Topics in Organometallic Chemistry)*, Springer, Berlin, **2006**.

[4] a) L. Jafarpour, S. P. Nolan, *Organometallics* **2000**, *19*, 2055–2057; b) L. Jafarpour, A. C. Hillier, S. P. Nolan, *Organometallics* **2002**, *21*, 442–444.

[5] a) A. J. Arduengo, J. C. Calabrese, D. Davidson, H. V. R. Dias, J. R. Goerlich, R. Krafczyk, W. J. Marshall, M. Tamm, R. Schmutzler, *Helv. Chim. Acta* **1999**, *82*, 2348; b) T. M. Trnka, J. P. Morgan, M. S. Sanford, T. E. Wilhelm, M. Scholl, T.-L. Choi, S. Ding, M. W. Day, R. H. Grubbs, *J. Am. Chem. Soc.* **2003**, *125*, 2546; c) G. W. Nyce, S. Csihony, R. M. Waymouth, J. L. Hedrick, *Chem. Eur. J.* **2004**, *10*, 4073–4079.

[6] a) M. S. Sanford, J. A. Love, R. H. Grubbs, *Organometallics* **2001**, *20*, 5314–5318; b) T. M. Trnka, E. L. Dias, M. W. Day, R. H. Grubbs, *ARKIVOC* **2002**, *13*, 28–41.

[7] Evaluating Ru–P and Ru–N bond lengths in complexes **9**[6b] and **10**[21] led to the conclusion that the indenylidene ligand has a stronger electron-donating ability than monosubstituted alkylidenes.

[8] M. Ulman, R. H. Grubbs, *J. Org. Chem.* **1999**, *64*, 7202–7207.

[9] T. Ritter, A. Hejl, A. G. Wenzel, T. W. Funk, R. H. Grubbs, *Organometallics* **2006**, *25*, 5740–5745.

[10] S. E. Lehman, K. B. Wagner, *Organometallics* **2005**, *24*, 1477–1482.

[11] Although the spontaneous formation of dimetallic complexes from **8b** has not been described, it is known from the literature that dimetallic systems can be formed, for example, a) E. L. Dias, R. H. Grubbs, *Organometallics* **1998**, *17*, 2758–2767; b) T. Weskamp, F. J. Kohl, W. Hieringer, D. Gleich, W. A. Herrmann, *Angew. Chem. Int. Ed.* **1999**, *38*, 2416–2419.

Received: August 23, 2007
Published Online: November 15, 2007

  